

# Phase Composition, Crystallite Size and Physical Properties of B<sub>2</sub>O<sub>3</sub>-added Forsterite Nano-ceramics

S Pratapa<sup>1</sup>, A Chairunnisa<sup>1</sup>, U Nurbaiti<sup>1,2</sup>, W D Handoko<sup>1</sup>

1 Department of Physics, Faculty of Mathematics and Sciences, Institute of Technology Sepuluh November (ITS), Jl. Arief Rahman Hakim, Surabaya 60111, Indonesia

2 Department of Physics, Faculty of Mathematics and Natural Sciences, Semarang State University, Jl. Raya Sekaran Gunung Pati, Semarang 50221, Indonesia

**Abstract.** This study was aimed to know the effect of B<sub>2</sub>O<sub>3</sub> addition on the phase composition, crystallite size and dielectric properties of forsterite (Mg<sub>2</sub>SiO<sub>4</sub>) nano-ceramics. It utilized a purified silica sand from Tanah Laut, South Kalimantan as the source of (amorphous) silica and a magnesium oxide (MgO) powder. They were thoroughly mixed and milled prior to calcination. The addition of 1, 2, 3, and 4 wt% B<sub>2</sub>O<sub>3</sub> to the calcined powder was done before uniaxial pressing and then sintering at 950 °C for 4 h. The phase composition and forsterite crystallite size, the microstructure and the dielectric constant of the sintered samples were characterized using X-ray diffractometer (XRD), Scanning Electron Microscope (SEM) and Vector Network Analyzer (VNA), respectively. Results showed that all samples contained forsterite, periclase (MgO) and proto enstatite (MgSiO<sub>3</sub>) with different weight fractions and forsterite crystallite size. In general, the weight fraction and crystallite size of forsterite increased with increasing B<sub>2</sub>O<sub>3</sub> addition. The weight fraction and crystallite size of forsterite in the 4%-added sample reached 99% wt and 164 nm. Furthermore, the SEM images showed that the average grain size became slightly larger and the ceramics also became slightly denser as more B<sub>2</sub>O<sub>3</sub> was added. The results are in accordance with density measurements using the Archimedes method which showed that the 4% ceramic exhibited 1.845 g/cm<sup>3</sup> apparent density, while the 1% ceramic 1.681 g/cm<sup>3</sup>. We also found that the higher the density, the higher the average dielectric constant, i.e. it was 4.6 for the 1%-added sample and 6.4 for the 4%-added sample.

## 1. Introduction

Forsterite (Mg<sub>2</sub>SiO<sub>4</sub>) can be considered as a functional material since it has a wide range potential of applications. Their interesting physical properties such as high melting point (approximately 1850 °C), low thermal expansion (below  $2 \times 10^{-5}$  °C<sup>-1</sup>) [1], good chemical stability and high-temperature thermal insulation [2] make suitable for refractory component. Moreover, pure forsterite is known to exhibit thermal expansion behavior which fits in the solid oxide fuel cell (SOFC) system as it is comparable to that of the SOFC components [3]. Forsterite also has low dielectric constants ( $\epsilon'$  of 6.5 and  $\epsilon''$  at an order of  $10^{-4}$ ) which match the requirement for microwave communication [4,5].

Forsterite solid ceramics were produced by several methods, including microwave sintering [6] and solid-state reaction [3]. The raw materials can be commercial magnesia products and commercial silica products [6, 7] or silica from natural sources [3,8]. There have been syntheses of nano-forsterite powders [9-11] in the literature, none of nano-forsterite ceramics, particularly those which were made from silica sand as the silica source.



Boria ( $B_2O_3$ ) has been used as a sintering agent to favor the densification of ceramics during sintering [7,12]. Since boria melts at 480 °C, sintering a boria-containing nano-forsterite compacted powder at high temperature is a strategy to obtain nano-forsterite ceramics. Provided the sintering temperature is below the reaction temperature between boria and the components of the ceramics, an improved densification can be expected without significant grain or crystallite growth of the major phase. Here, we report the synthesis and characterization of boria-added forsterite nano-ceramics. The raw materials were commercial magnesia and Indonesia local sand-derived silica. The effects of boria addition on the phase composition, density-porosity, crystallite and grain sizes, and dielectric constant of the forsterite ceramics were examined.

## 2. Materials and methods

This research used a purified natural silica sand which was taken from Tanah Laut, South Kalimantan as the source of silica and MgO powder (Merck) which contained some magnesium hydroxide ( $Mg(OH)_2$ ). The silica sand was purified through screening-washing, milling, magnetic separation, immersion in a 2M chloride acid finally drying at room temperature to obtain a white silica powder. This powder was further processed with reaction using NaOH to obtain  $NaSiO_3$  and then titration with HCl to gain amorphous silica powder. The water in the MgO powder was removed by heating at 400 °C for 30 mins. The amorphous silica and the treated MgO powders at a molar ratio of 1:2 were then mixed with 3 wt% addition of poly(vinyl) alcohol through ball milling for 3 h. The mixture was calcined at 950 °C for 1 h to produce forsterite nanopowder. Manual grinding was applied to the powder to give finer forsterite powder, mixed with  $B_2O_3$  powder at 1, 2, 3 and 4% by weight as a sintering agent. The sintering was done to the uniaxially-pressed powders at 950 °C for 4 h to produce  $B_2O_3$ -added forsterite nano-ceramics.

The phase analyses were applied to the laboratory x-ray diffraction (XRD) data which were collected from all ceramic samples using an Empyrean PANalytical XRD. The XRD used a Cu target and was operated at 40 kV and 30 mA with  $2\theta$ -range between 15 and 65°  $2\theta$  and 0.017 °  $2\theta$  step-size. The phase composition analysis on the XRD data was done using Rietica software [13].

The characterizations of the ceramics included diameter shrinkage, porosity and density, Vickers hardness, thermal expansion and dielectric constant. The porosity and density of the ceramics were determined using the Archimedes method following the Australian Standard No. 1774.5-2014. A transmission phase-shift method has been employed to an Advantest R3770 vector network analyzer connected to an A-INFOMW WG P/N 90WCAN rectangular waveguide to acquire the dielectric properties of the ceramics at a microwave frequency from 8 – 12 GHz. SEM micrographs were also collected from the fractured surface of the sintered ceramics using FEI Inspect-S50.

## 3. Results and discussion

Figure 1 presents the XRD pattern ( $CuK\alpha$  radiation) of the calcined powder. Phase identification showed that the powder contained forsterite ( $Mg_2SiO_4$ ), proto-enstatite ( $MgSiO_3$ ), periclase (MgO) which referred to PDF number 34-189,3-523, 43-1022 respectively. Further analysis using Rietveld 'ZMV' method revealed that the corresponding weight fractions of these phases were 86.8, 9.9, and 3.2%. It means, the synthesis has produced forsterite as the dominating phase through presumably direct reaction of  $2MgO+SiO_2 \rightarrow Mg_2SiO_4$ . Meanwhile, proto-enstatite was yielded through  $MgO+SiO_2 \rightarrow MgSiO_3$ . These results indicate that the reaction between silica and magnesia (a) was incomplete since there was some magnesia excess and (b) occurred in a non-homogeneous mixture. The latter can be concluded from the fact that forsterite, proto-enstatite, and periclase are simultaneously identified in the powder. This powder synthesis result is in accordance with such a forsterite synthesis where quartz powder was used as the raw material [3]. Further analysis using MAUD software, after an instrument broadening correction, showed that this powder exhibited a crystallite size of approximately 100 nm. Therefore, a relatively high content, nanometric forsterite powder has been successfully produced using the method mentioned above.

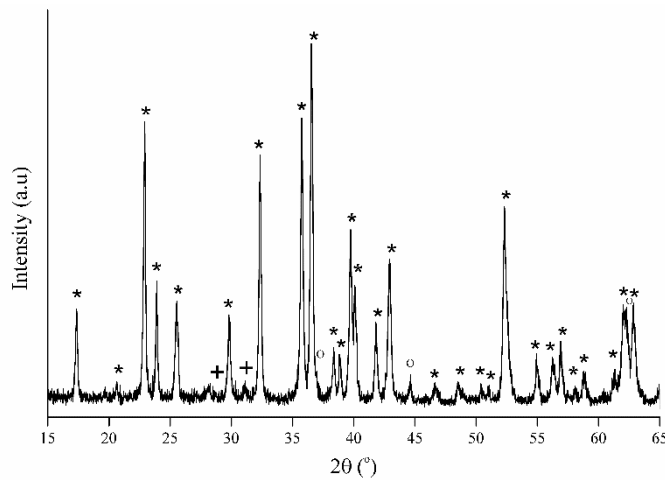


**Figure 1.** XRD pattern (CuK $\alpha$  radiation) of the calcined powder.

\* = forsterite (Mg<sub>2</sub>SiO<sub>4</sub>); + = proto-enstatite (MgSiO<sub>3</sub>);

o = periclase (MgO).

Then, XRD data analyses were done to provide the structure, the phase composition and the crystallite size information of forsterite in the sintered ceramics – the patterns are shown in Figure 2. In general, the ceramics contained only forsterite and periclase, except the 1%-added (A) sample which also had proto-enstatite. The figure shows the diminishing of proto-enstatite and reducing peak intensity of periclase, which, in general, suggests that the amount of added boria affects the formation of forsterite. Table 1 displays the weight fraction of forsterite in the B<sub>2</sub>O<sub>3</sub>-added nano-forsterite ceramics. It is obvious that addition of 4 wt% of boria results in a nearly pure forsterite ceramic, which is not achieved in the powder. It is argued, then, that boria has favored the formation of forsterite. Sintering at 950 °C for 4 h allowed the melted boria to homogenize the distribution of the silica (or more exactly the proto-enstatite) and magnesia particles to form forsterite through MgO+MgSiO<sub>3</sub>→Mg<sub>2</sub>SiO<sub>4</sub>. The results also imply that besides the identified periclase crystallites there should be some amorphous silica excess in the ceramic samples. To summarize, the addition of boria caused the improvement of the forsterite formation in the ceramics.

Table 1 also presents the crystallite size of forsterite from further XRD data analyses of the ceramics. The addition of boria from 1% to 4% has increased the crystallite size from 104 nm to 164 nm. It appears that the boria addition cannot fully withstand the crystallite growth of forsterite. The presence of melted boria during sintering not only homogenized the distribution of particles from different phases but also promoted crystallite growth of the same phase. Nevertheless, the 4% sample still exhibited sub-nanometric characteristics.

The density-porosity characters of the ceramics are also presented in Table 1. An increase in density (therefore a decrease in porosity) with the addition of boria is evident. It is worthing to note that the ceramics are still very porous, presumably due to the low sintering temperature. Figure 3 shows the SEM micrographs which support this results. Reduction of porosity is apparent but not significant.

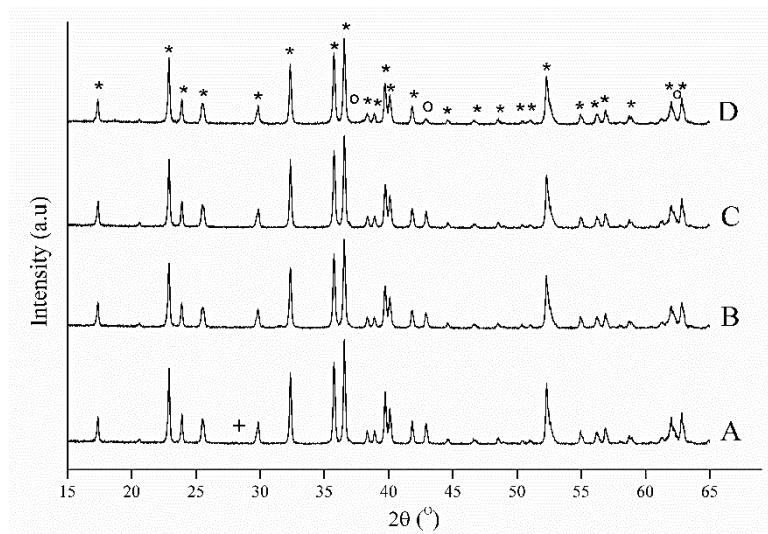


**Figure 2.** XRD pattern (CuK $\alpha$  radiation) of the B<sub>2</sub>O<sub>3</sub>-added ceramics.

\* = forsterite (Mg<sub>2</sub>SiO<sub>4</sub>); + = proto-enstatite (MgSiO<sub>3</sub>);  
o = periclase (MgO).

**Table 1.** Weight fraction and crystallite size of forsterite in the B<sub>2</sub>O<sub>3</sub>-added nano-forsterite ceramics and their apparent density-porosity characteristics.

Sample	Weight Fraction (%)			Crystallite size (nm)	Density (g/cm <sup>3</sup> )	Porosity (%)
	Forsterite	Periclase	Proto-enstatite			
A	95.3±0.7	4.5±0.3	0.2	104±13	1.68	44.3
B	95.6±0.8	4.4±0.3	0.0	110±6	1.70	38.2
C	95.7±0.3	4.3±0.3	0.0	118±19	1.82	36.9
D	99.1±0.8	0.9±0.1	0.0	164±24	1.85	25.5

Considering higher sintering temperature is possible, yet the crystallite size would be sacrificed as a result of a synthesis trade-off.

Figure 4 depicts the dielectric constant  $\epsilon_r$  plots against frequency of the ceramics. Clearly, the dielectric constant of the ceramics is frequency-dependent. There are, for example, three distinct peaks for each sample at 8.4, 10.5 and 11.5 GHz. Moreover, the ranges of the dielectric constant value are 4.0-7.5, 4.0-7.5, 4.5-7.5 and 4.5-7.8 for sample A, B, C, and D respectively. The average dielectric constant was 4.6 for the 1%-added sample and 6.4 for the 4%-added sample. These ranges are slightly different and their fluctuations are insignificant. In addition, these values are low, as also found by others [3,14,15]. Therefore, the ceramics exhibited dielectric properties which make them appropriate for millimeter-wave communication applications.

#### 4. Conclusions

This study showed that forsterite-based nano-ceramics can be synthesized via a solid reaction between amorphous silica, which was derived from natural silica sand, and magnesia powders. The nano-metric size of the forsterite can be retained with the largest size reached a value of 164 nm after 4 wt% boria addition. The addition also caused a significant increase in the weight fraction of forsterite and a decrease in porosity. Interestingly, although slightly frequency-dependent, the real dielectric constant of the ceramics are similar in their values.

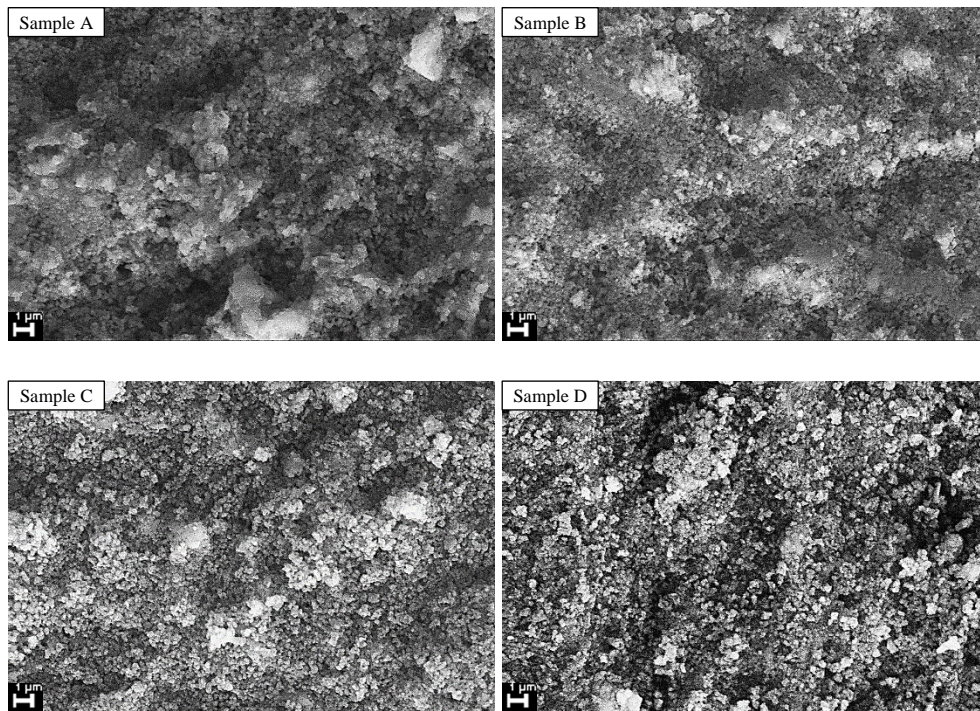


**Figure 3.** SEM micrographs of fractured surface of the B<sub>2</sub>O<sub>3</sub>-added ceramics.

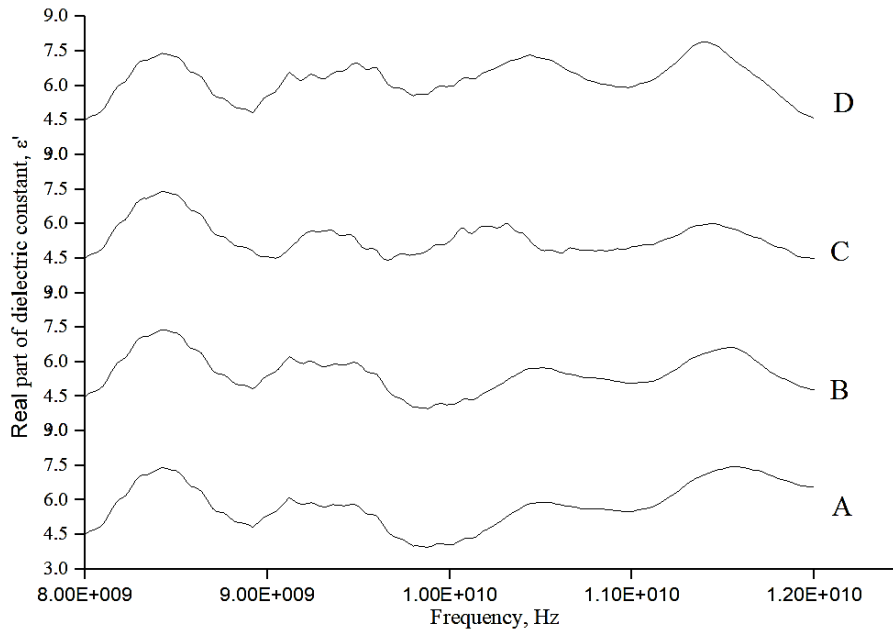


**Figure 4.** Frequency-dependent dielectric constant  $\epsilon_r$  of the B<sub>2</sub>O<sub>3</sub>-added ceramics.

## 5. References

- [1] Choudhury N, Chaplot S L and Rao K R 1989 Equation of state and melting point studies of forsterite *Phys Chem Minerals* **16** 599–605

- [2] Delvaux P, Desrosiers L and Gouin M 1991 Forsterite and its use as insulating material *US Patent No US4985164 A*
- [3] Pratapa S, Handoko W D, Nurbaiti U and Mashuri 2017 Synthesis and characterization of high-density B<sub>2</sub>O<sub>3</sub>-added forsterite ceramics *Ceramics International* **43** 7172–6
- [4] Ohasto H, Tsunooka T, Ando M, Ohishi Y, Miyauchi Y and others 2003 Millimeter-wave dielectric ceramics of alumina and forsterite with high quality factor and low dielectric constant *Journal of the Korean Ceramic Society* **40** 350–3
- [5] Tsunooka T, Ando M, Suzuki S, Yasufuku Y and Ohsato H 2013 Research & developments for millimeter-wave dielectric forsterite with low dielectric constant, high Q, and zero temperature coefficient of resonant frequency *Japanese Journal of Applied Physics* **52** 09KH02
- [6] Barzegar Bafrooei H, Ebadzadeh T and Majidian H 2014 Microwave synthesis and sintering of forsterite nanopowder produced by high energy ball milling *Ceramics International* **40** 2869–76
- [7] Fan G, Zhou H and Chen X 2016 Optimized sintering temperature and enhanced microwave dielectric performance of Mg<sub>2</sub>B<sub>2</sub>O<sub>5</sub> ceramic *J Mater Sci: Mater Electron* 1–5
- [8] Reaney I M, Wise P, Uvic R, Breeze J, Alford N M, Iddles D, Cannell D and Price T 2001 On the temperature coefficient of resonant frequency in microwave dielectrics *Philosophical Magazine A* **81** 501–10
- [9] Fathi M H and Kharaziha M 2008 Mechanically activated crystallization of phase pure nanocrystalline forsterite powders *Materials Letters* **62** 4306–9
- [10] Kamran A H R, Moztarzadeh F and Mozafari M 2011 Synthesis and characterization of high-pure nanocrystalline forsterite and its potential for soft tissue applications *Advanced Composites Letters* **20** 41–7
- [11] Saberi A, Alinejad B, Negahdari Z, Kazemi F and Almasi A 2007 A novel method to low temperature synthesis of nanocrystalline forsterite *Materials Research Bulletin* **42** 666–73
- [12] Liu C-Y, Tsai B-G, Weng M-H and Huang S-J 2013 Influence of B<sub>2</sub>O<sub>3</sub> additive on microwave dielectric properties of Li<sub>2</sub>ZnTi<sub>3</sub>O<sub>8</sub> ceramics for LTCC applications *International Journal of Applied Ceramic Technology* **10** E49–56
- [13] B.A. Hunter, Rietica, newsletter of international union of crystallography, *Comm.Powder Diffr.* 20 (1998) 21
- [14] Bernardo E, Fiocco L, Giffin G A, Di Noto V and Colombo P 2014 Microstructure development and dielectric characterization of forsterite-based ceramics from silicone resins and oxide fillers *Advanced Engineering Materials* **16** 806–13
- [15] Sano S, Saito N, Matsuda S-I, Ohashi N, Haneda H, Arita Y and Takemoto M 2006 Synthesis of high density and transparent forsterite ceramics using nano-sized precursors and their dielectric properties *Journal of the American Ceramic Society* **89** 568–74

### Acknowledgement

We are indebted to the Ministry of Research Technology and Higher Education of the Republic of Indonesia and Institute for Research and Community Services ITS Surabaya for the support of research funding provided to SP through the PUPT-2016 No. 01751/IT2.11/PN.08/2016 and PBK-2017 No. 528/PKS/ITS/2017.